Biochemical and Biophysical Research Communications 433 (2013) 139–144

Contents lists available at SciVerse ScienceDirect

Biochemical and Biophysical Research Communications

journal homepage: www.elsevier.com/locate/ybbrc

A hypoxia-inducible factor (HIF)-3α splicing variant, HIF-3α4 impairs angiogenesis in hypervascular malignant meningiomas with epigenetically silenced HIF-3α4

Hitoshi Ando [a,b], Atsushi Natsume [a,*], Kenichiro Iwami [a], Fumiharu Ohka [a], Takahiro Kuchimaru [c], Shinae Kizaka-Kondoh [c], Kengo Ito [d], Kiyoshi Saito [b], Sachi Sugita [e], Tsuneyoshi Hoshino [e], Toshihiko Wakabayashi [a]

[a] Department of Neurosurgery, Nagoya University School of Medicine, Nagoya, Japan
[b] Department of Neurosurgery, Fukushima Medical University School of Medicine, Fukushima, Japan
[c] Department of Biomolecular Engineering, Tokyo Institute of Technology Graduate School of Bioscience and Biotechnology, Yokohama, Japan
[d] National Center for Geriatrics and Gerontology, Aichi, Japan
[e] MICRON Inc.Medical Facilities Support Department, Aichi, Japan

ARTICLE INFO

Article history:
Received 13 February 2013
Available online 26 February 2013

Keywords:
Hypoxia-inducible factor-3α4
Brain tumor
Angiogenesis
Metabolism

ABSTRACT

Hypoxia inducible factor is a dominant regulator of adaptive cellular responses to hypoxia and controls the expression of a large number of genes regulating angiogenesis as well as metabolism, cell survival, apoptosis, and other cellular functions in an oxygen level-dependent manner. When a neoplasm is able to induce angiogenesis, tumor progression occurs more rapidly because of the nutrients provided by the neovasculature. Meningioma is one of the most hypervascular brain tumors, making anti-angiogenic therapy an attractive novel therapy for these tumors. HIF-3α has been conventionally regarded as a dominant-negative regulator of HIF-1α, and although alternative HIF-3α splicing variants are extensively reported, their specific functions have not yet been determined. In this study, we found that the transcription of HIF-3α4 was silenced by the promoter DNA methylation in meningiomas, and inducible HIF-3α4 impaired angiogenesis, proliferation, and metabolism/oxidation in hypervascular meningiomas. Thus, HIF-3α4 could be a potential molecular target in meningiomas.

1. Introduction

Brain tumors are classified into grades I–IV by the World Health Organization (WHO) according to histological features, with grade I being the most benign and grade IV being the most severe. Meningiomas are frequent neoplasms accounting for approximately 25% of all intracranial tumors [11]. They are mainly characterized by a benign histology and an indolent clinical course, and most are pathologically diagnosed as WHO grade I and curable by surgical resection. However, grade II or III meningiomas are occasionally encountered. Even more troublesome, some populations of meningiomas with benign pathological findings (WHO grade I) pursue a malignant course [12–14]. Our group has previously reported the use of whole genome methylation analysis to predict which tumors will undergo this malignant clinical course, and we were able to predict the outcome in meningioma patients on the basis of the methylation status of 5 hub genes, including HIF-3α [15].

When a neoplasm is able to induce angiogenesis, tumor progression occurs more rapidly because of the nutrients provided by the neovasculature [1–3]. Meningioma is one of the most hypervascular tumors, making anti-angiogenic therapy an attractive novel therapy for these tumors [16]. This therapy targets angiogenetic factors, including vascular endothelial growth factor (VEGF) and platelet-derived growth factor, both of which are regulated by hypoxia inducible factor (HIF) [4,17,18].

HIF is a dominant regulator of adaptive cellular responses to hypoxia and controls the expression of a large number of genes regulating angiogenesis as well as metabolism, cell survival, apoptosis, and other cellular functions in an oxygen level-dependent manner. HIF forms a dimer consisting of an unstable α subunit (HIF-α) and a stable β subunit (HIF-β). This dimer binds to specific sequences termed hypoxia response elements (HRE) in the promoter region of HIF target genes such as VEGF. There are 3 principal isoforms of the HIF-α subunit (HIF-1α, 2α, 3α). HIF-1α and HIF-2α share a similar domain architecture and undergo similar proteolytic regulation [4–6,10,17,19,20]. HIF-3α, on the other hand, has been

* Corresponding author. Address: Department of Neurosurgery, Nagoya University School of Medicine, 65 Tsurumai-cho, Showa-ku, Nagoya 466-8550, Japan. Fax: +81 52 744 2360.
E-mail address: anatsume@med.nagoya-u.ac.jp (A. Natsume).

0006-291X/$ - see front matter © 2013 Elsevier Inc. All rights reserved.
http://dx.doi.org/10.1016/j.bbrc.2013.02.044

conventionally regarded as a dominant-negative regulator of HIF-1α [4–10], and although alternative HIF-3α splicing variants are extensively reported, their specific functions have not yet been determined [5,7,8,10,21]. HIF-3α4, one of the HIF-3α splicing variants, is similar to mouse inhibitory Per/Arnt/Sim domain protein (IPAS). IPAS expression in hepatoma cells selectively impairs tumor vascular density, and inhibition of IPAS expression induces vascular growth in the cornea of mice [9].

In this study, we constructed a meningioma cell line stably expressing HIF-3α4 in order to elucidate the function of HIF-3α4 in hypervascular malignant meningioma. We addressed multiple novel functions of HIF-3α4 in hypervascular meningiomas; angiogenesis, proliferation, and metabolism/oxidation. HIF-3α4 could be a potential molecular target in meningiomas.

2. Materials and methods

2.1. Cell lines

The human meningioma cell lines IOMM-Lee and HKBMM were kindly provided by Drs. Anita Lai (University of California at San Francisco, CA) and Shinichi Miyatake (Osaka Medical University, Osaka, Japan), respectively. All cell lines were maintained in Dulbecco's modified Eagle medium (DMEM) containing 10% fetal bovine serum (FBS) and 1% penicillin/streptomycin. Cell lines were grown at 37 °C in a humidified atmosphere of 5% CO_2 under normoxic (20% O_2) or hypoxic (1% O_2) conditions.

2.2. Genetically engineered meningioma cells

Using the following protocol, we designed IOMM-Lee or HKBMM meningioma cell lines stably expressing green fluorescence protein (GFP) or GFP-tagged HIF-3α4, designated IO-GFP, IO-HIF3α4, HK-GFP, and HK-HIF3α4, respectively. pQCXIP-HIF3α4-GFP plasmid was prepared by the following protocol: HIF-3α transcript variant 3, isoform c complete cDNA (accession No. BC080551) was obtained from GeneCopoeia (Rockville, MD). This cDNA was amplified using the forward primer 5′-CTAGATGAATTCATGGCGCTGGGGCTGCAGCG-3′, including an *Eco*RI site and the reverse primer 5′-CTAGATCGCGGCCGCTCAGCTCAGCAAGGTGTGGATGC-3′, including a *Not*I site. Oligonucleotides were obtained from Greiner Japan (Tokyo, Japan). After amplification, the products were purified by a QIAquick® Spin kit (QIAGEN, Hilden, Germany) and sequenced on an automated DNA sequencer (ABI PRISM 310, Applied Biosystems, Foster City, CA). Then, the products were digested by *Eco*RI and *Not*I (Takara Bio, Otsu, Japan), and the DNA was inserted to pQCXIP retrovirus vector (Clontech, Mountain View, CA) that had previously been altered to contain the GFP gene by using the DNA Ligation kit (Takara Bio, Otsu, Japan). These plasmids were co-transfected with pVSV-G (Clontech) into the retroviral packaging cell line 293T using Lipofectamine 2000 reagent (Invitrogen, Carlsbad, CA) to produce retrovirus. At 24 h post-transfection with pQCXIP-HIF3α4-GFP and pVSV-G, the medium was changed to DMEM. After another 24 h, the supernatant containing viral particles was collected and filtered through a 0.45-μm-pore PVDF membrane filter (Millex®-HV Syringe Driven Filter Unit; Millipore, Bradford, MA). IOMM-Lee or HKBMM meningioma cells were incubated for 48 h with the viral supernatant plus 4 μg/mL polybrene infection/transfection reagent (Millipore). Cells were then treated with 10 μg/mL puromycin (Sigma–Aldrich, St. Louis, MO) for 1 week to select the cells stably expressing HIF-3α4 and GFP.

2.3. Demethylation treatment

Cells (1×10^5 cells) were seeded in 6-well plate and incubated for 24 h, then treated with 5-aza-2′-deoxycytidine at the final concentration of 0, 1 or 5 μM. After the first administration, the same dose agent was added four times in total every 12 h. At 12 h after the fourth administration, medium was changed, and cells then were collected and RNA was extracted.

2.4. RNA extraction, reverse transcriptase PCR, and quantitative real-time PCR

RNA was extracted from IOMM-Lee or HKBMM cell line using Trizol® (Invitrogen, Carlsbad, CA). The following gene-specific oligonucleotide primers were obtained from Greiner Japan: HIF-1α forward 5′-GAGCTTGCTCATCAGTTGCC-3′ and reverse 5′-CTGTA CTGTCCTGTGGTGAC-3′, and HIF-3α4 forward 5′-CCCAGAGCTCAGAGGACGAG-3′ and reverse 5′-CCCAACACACCAGGCTGAGA-3′. First-strand cDNA was synthesized by Transcriptor First Strand cDNA synthesis kit (Roche, Indianapolis, IN) according to the manufacturer's instructions. The resulting products were analyzed on a 2% agarose gel stained with ethidium bromide. Quantitative real-time PCR (qPCR) was performed using the LightCycler 480 system (Roche Applied Science, Mannheim, Germany) and the Light Cycler 480 SYBR Green I Master (Roche).

2.5. Antibodies

Anti-HIF-1α antibody and anti-HIF-3α antibody were obtained from Novus Biologicals (Littleton, CO). Anti-GFP antibody was from MBL (Nagoya, Japan). Anti-β-actin antibody was from Sigma–Aldrich.

2.6. Protein extracts and western blot analysis

Meningioma cell lysates were prepared by lysing cells in 200 μL of 2× lysis buffer (20% [v/v] glycerol, 13.5% [v/v] 1 M Tris–HCl, 40% [v/v] 10% SDS, 4.0 ng bromophenol blue, 10% [v/v] mercaptoethanol, 16.5% [v/v] water). Lysates (10 μL) were loaded into 10% Mini-PROTEAN TGX Gels (BIO-RAD, Hercules, CA). Separated proteins were electrotransferred onto PVDF membranes (Hybond-P, GE Healthcare, Buckinghamshire, United Kingdom); then, western blots were performed using the antibodies listed above. Bands were detected using ECL Western Blotting Detection Reagents (GE Healthcare).

2.7. Protein interaction assay

Meningioma cells were seeded in 10-cm cell culture dishes and lysed in TNE buffer (150 mM NaCl, 35 mM Tris–HCl, 1% NP-40, 1 mM EDTA, 10 μg/mL aprotinin) at 4 °C. The lysates were immunoprecipitated with the anti-GFP antibody bound to Pierce® Protein G Agarose (Thermo Scientific, Rockford, IL) according to the manufacturer's instructions. The immunoprecipitated samples were analyzed by western blotting as described above.

2.8. Wound scratch assay

Meningioma cells were seeded in 10-cm tissue culture dishes at a concentration of 30×10^4 cells/mL and cultured under normoxia or hypoxia. Linear wounds were generated in the monolayer with the tips of a sterile 200-μL plastic pipette. Cellular debris was removed by washing with phosphate buffered saline (PBS). PBS was removed, and DMEM supplemented with 2% [v/v] FBS and 1% [v/v] penicillin–streptomycin was added to the culture dishes. Every 6 h, wounds were photographed at 20 scratched points per dish and each wound area was estimated using Image J software (Rasband, W.S., Image J, National Institutes of Health, Bethesda, MD, http://rsb.info.nih.gov/ij/, 1997–2009).

2.9. Cell growth assay

Cells were seeded in 96-well plates at 1×10^3 cells/well. At 24 and 48 h after plating, the cells were treated using the Cell counting Kit-8 (Dojindo, Kumamoto, Japan), and the absorbance was examined by Multi Label Reader 2030 ARVO X4 (Perkin Elmer, Waltham, MA).

2.10. Quantification of tumor vessels and overall survival time

All animal experiments were conducted in accordance with the Faculty of medicine of Nagoya University. IO-GFP or IO-HIF3α4 cells, 3×10^5 cells/2 μL were stereotactically injected into the brain of Balb-c nu/nu nude mice (female, 5 weeks of age) under anesthesia using a Hamilton syringe (Hamilton, Reno, NV). The coordination was 1.4 mm posterior from bregma, 3.0 mm to the right, at a 4.0-mm depth from brain surface. The overall survival was measured for up to 40 days. Five minutes before the mice were euthanized, animals were perfused with 0.5 mL of 10 g/L 155 kDa tetramethylrhodamine isothiocyanate-dextran (tetramethylrhodamine) (Sigma–Aldrich). Tumor-bearing brains were rapidly removed and fixed in 4% paraformaldehyde at 4 °C for 24 h. Coronal sections (100 μm thick) were cut on a vibratome, and the samples were examined by a laser scanning confocal microscope (FV1000-D; Olympus, Tokyo, Japan). The vessels that were enhanced by tetramethylrhodamine in the region of interest (ROI) in the tumor were visible by the presence of green fluorescence from GFP, and these areas were scanned in a 521 × 521 pixel format in the *x*–*y* direction of the ROI using a ×10 frame scan and 16 optical sections along the *Z*-axis with a 50-μm step. After collecting the data from the vessels from 10 ROIs, the data were imported as binary and reconstructed to three-dimensional images. The number of vascular voxels per total voxels of the ROI was calculated. The processing was performed using Image J software.

2.11. Positron emission computerized-tomography (PET) imaging

Meningioma IO-GFP or IO-HIF3α4 cells (1×10^6 in 100 μL PBS) were injected subcutaneously into the left shoulder of Balb-c nu/nu nude mice (female, 5 weeks of age) under anesthesia. When the tumor size reached about 100 mm^3, PET examination was performed as follows: After 24 h fasting, 20 MBq/200 μL fluorodeoxyglucose (FDG) was intravenously injected under inhalational anesthesia. PET imaging was performed 60 min after this treatment, and accumulation of FDG was measured for 30 min. After 48 h FDG-PET examination, 7.5 MBq/200 μL fluoromisonidazole (FMISO) was administered to mice. After 90 min of free movement, inhalational anesthesia was introduced, and the accumulation of FMISO was measured for 30 min.

2.12. Statistical analysis

Data are expressed as mean ± SEM. Comparison of treatments against controls was made using one-way ANOVA followed by Fisher's LSD post hoc test using SPSS version 19 (IBM, Chicago, IL). *P* values of <0.05 were considered significant. The duration of overall survival were analyzed in the Kaplan–Meier format using the log-rank test for statistical significance.

3. Results

3.1. Hypoxia induces the expression of HIF-3α4

We previously demonstrated that HIF-3α4 was a DNA-methylated gene useful in predicting the outcome of meningiomas. As predicted, the expression of HIF-3α4 was not detected in untreated meningioma cell lines. By contrast, IOMM-Lee cell line expressed similarly high amounts of HIF-1α under normoxic and hypoxic conditions (Fig. 1A). A DNA-demethylating agent, 5-aza-2′-deoxycytidine, induced the expression of HIF-3α4 (Fig. 1B), suggesting that the transcription of HIF-3α4 is silenced by DNA methylation under normal conditions.

HIF-3α4, one of the HIF-3α splicing variants, is similar to mouse IPAS. It was of great interest to investigate how overexpression of HIF-3α4 affects the interaction between HIF-1α and angiogenesis in hypervascular meningioma. Therefore, we successfully generated GFP-tagged stable transfectants expressing HIF-3α4 (Fig. 1C). The finding was also consistent with another genetically-engineered cell line, HK-HIF3α4 (data not shown).

3.2. HIF-3α4 binds to HIF-1α

Previous reports showed that HIF-3α4 forms an abortive transcriptional complex with HIF-1α and prevents the engagement of HIF-1 to the HREs located in the promoter/enhancer regions of hypoxia-inducible genes [4,17,18]. In this study, cell lysate from IOMM-Lee cells stably expressing GFP-tagged HIF-3α4 (IO-HIF-3α4) was immunoprecipitated with anti-GFP antibody and then subjected to western blotting with anti-HIF-1α antibodies. As shown in Fig. 1D, western blotting with anti-HIF-1α detected a band corresponding to 93-kDa HIF-1α in the immunoprecipitated lysate from IO-HIF-3α4 but not in that from the control IO-GFP lysate. Consistent with the previous reports, this experiment demonstrated that HIF-3α4 binds to HIF-1α in meningioma.

Next, we investigated whether HIF-3α4 enhanced the transcription of hypoxia-inducible genes. The transcription of VEGF was markedly suppressed in IO-HIF-3α4 cells compared to IO-GFP cells (Fig. 1E).

3.3. HIF-3α4 directly inhibits the proliferation and invasion of meningioma cells

The HIF family is multifactorial; it regulates angiogenesis, metabolism, proliferation, and invasion/metastasis [20]. However, little is known about the function of HIF-3α4 in tumor cells. Overexpression of HIF-3α4 significantly retarded cell proliferation under normoxia and hypoxia (Fig. 2A). In scratch wound healing assay, healing speed was slower in IO-HIF-3α4 cells than in IO-GFP ($P < 0.05$, Fig. 2B), suggesting that HIF-3α4 inhibits proliferation and invasion in meningioma cells.

3.4. HIF-3α4 reduces neovascularization and glucose metabolism in meningioma

In order to visualize neovasculature in meningioma growing in the brain of mice, mice with GFP-tagged meningiomas were injected with tetramethylrhodamine (TMR). TMR-stained hyperdense vessels were observed in GFP-expressing tumors (Fig. 3A). Sequential images along the *Z*-axis allowed us to create three-dimensional images (Fig. 3B). The number of vascular voxels per total voxels of the ROI was calculated in IO-HIF-3α4 and IO-GFP meningiomas (Fig. 3C). Vascular density was significantly reduced in IO-HIF-3α4 tumors compared to IO-GFP tumors.

FDG, an analog of glucose, was used to generate PET images representing glucose metabolic activity in a region of tumor tissue. In clinical settings, the FDG uptake of the tumor and reference region (the tumor-to-gray matter ratio; TGR) is relatively high in meningioma, and is correlated with the tumor aggressiveness determined by the MIB-1 index [11]. While FDG uptake was high in the control IO-GFP tumors, it was significantly reduced in IO-HIF-3α4 tumors (Fig. 3D). FMISO is a nitroimidazole derivative, and

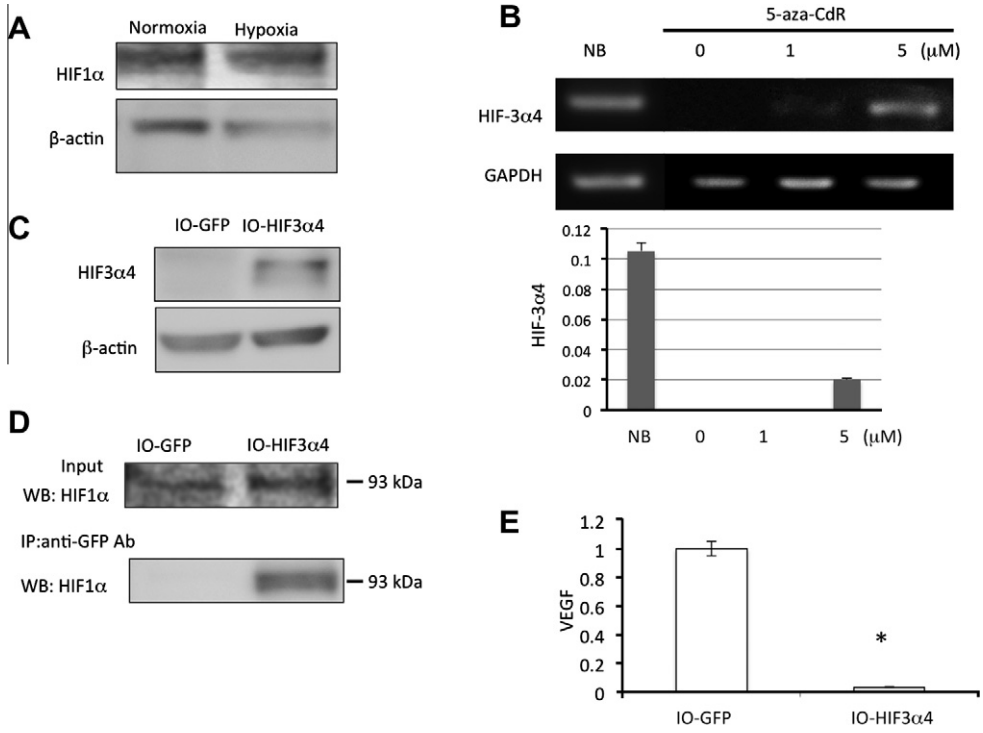

Fig. 1. (A) HIF-1α is constitutively expressed in IOMM-Lee meningioma cells under under normoxic and hypoxic conditions. (B) A DNA-demethylating agent, 5-aza-deoxycytidine (5-aza-CdR), induced the expression of HIF-3α4. (C) IOMM-Lee meningioma cells stably expressing GFP-tagged HIF-3α4 were generated through cloning and puromycin selection. (D) Lysates from IOMM-Lee cells stably expressing GFP or HIF-3α4 were immunoprecipitated using anti-HIF-1α antibody. We detected a band corresponding to 93-kDa HIF-1α in the immunoprecipitated lysate from IO-HIF-3α4, but not in that from the control IO-GFP. (E) The transcription of VEGF was markedly suppressed in IO-HIF-3α4 cells compared to IO-GFP cells.

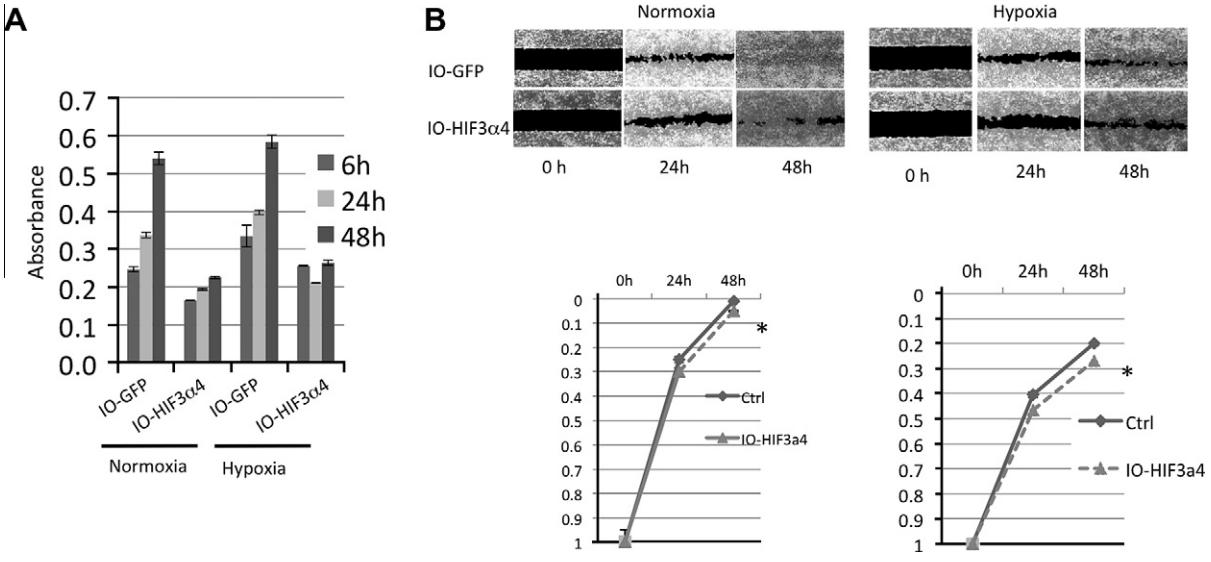

Fig. 2. HIF-3α4 directly inhibits the proliferation and invasion of meningioma cells. (A) Overexpression of HIF-3α4 significantly retarded cell proliferation under normoxia and hypoxia. (B) In scratch wound healing assay, the healing speed was slower in IO-HIF-3α4 cells than in IO-GFP cells ($P < 0.05$).

FMISO PET can image tumor hypoxia by increased FMISO tumor uptake, because FMISO metabolites are trapped exclusively by hypoxic cells [22]. In the control IO-GFP tumors, FMISO uptake was slightly higher than in the normal region. By contrast, HIF-3α4 overexpression markedly decreased FMISO uptake. As we discuss later, although HIF-3α4 reduced neovascularization (Fig. 3B), reduction of FMISO uptake in IO-HIF-3α4 tumors may have resulted from decreased tumor size, rather than HIF-3α4-mediated hypoxia. Indeed, there was a tendency toward correlation between FMISO uptake and tumor volume.

3.5. HIF-3α4 prolongs the survival time of mice with malignant meningiomas

IO-GFP or IO-HIF-3α4 cells (3×10^5 cells) were inoculated into the brain of nude mice. The animals with IO-GFP control tumors

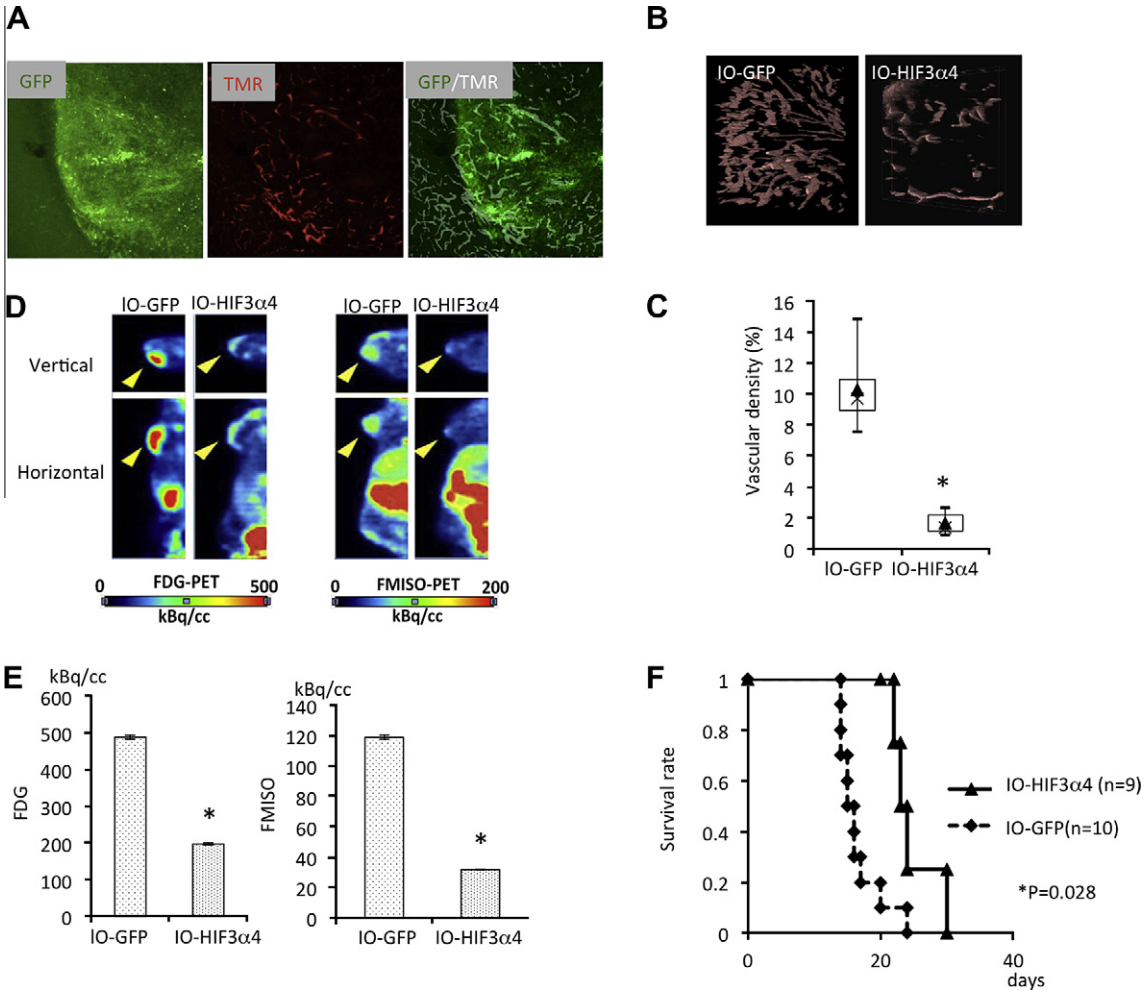

Fig. 3. HIF-3α4 reduced neovascularization and glucose metabolism in meningioma. (A) Tetramethylrhodamine (TMR)-stained hyper-dense vessels seen in GFP-expressing tumors. (B) Sequential images along the *Z*-axis enabled us to create three-dimensional images. (C) The number of vascular voxels per total voxels of the ROI was calculated in IO-HIF-3α4 and IO-GFP meningiomas. (D) FDG-PET (left) and FMISO-PET (right). While FDG uptake was extensively high in the control IO-GFP tumors, it was significantly reduced in IO-HIF-3α4 tumors. In the control IO-GFP tumors, FMISO uptake was slightly higher than the normal region. By contrast, overexpression of HIF-3α4 markedly decreased FMISO uptake.

died by 25 days after inoculation. However, the survival of mice with IO-HIF-3α4 tumors was prolonged significantly. This result suggests that the induction of HIF-3α4 was unable to cure mice with malignant meningiomas, but it did confer a survival advantage (Fig. 3F).

4. Discussion

First, the present study demonstrated that the HIF-1α expressed at considerable levels even under normoxic condition in IOMM-Lee meningioma cells. Taking into account that meningioma is one of the most hypervascular tumors, such levels of HIF-1α expression may be reasonable. The gene expression of endogenous HIF-3α4 appeared to be silenced probably due to DNA methylation [15]. Therefore the following experiments were performed under normoxia to assign a focus on the function of transfected HIF-3α4.

Previously, Heikkil et al. indicated that HIF-3α4 directly bound to HIF-1α to inhibit its transcriptional activity [10]. In the present study, we confirmed the interaction between GFP tagged HIF-3α4 and HIF-1α in IO-HIF3α4 cells by immunoprecipitation assay (Fig. 1D). Next we addressed the effect of HIF-3α4 on proliferation, invasion, angiogenesis, glucose-metabolism, and hypoxic state by cell growth assay, wound scratch assay, vascular imagings, FDG-PET, and FMISO-PET, respectively. As the results, all of these activities were decreased in IO-HIF3α4 cells (Figs. 2 and 3). As Rankin and Giaccia, and Semenza et al. reported, the expression of various genes such as VEGF, GLUT-1, EPO, E-CADHERIN and others, relevant to angiogenesis, metabolism, proliferation and invasion/metastasis, are regulated by HIF-1α [4,6,7,10,17,20,23]. Also, as mentioned above, I confirmed the interaction between HIF-1α and HIF-3α4 and the suppression of VEGF expression in IO-HIF3α4 cells. These results together suggest that overexpression of HIF-3α4 might inhibit transcription activity of HIF-1α. Since HIF-1α has many other target genes, their functions should also be examined in future. To clarify the function of HIF-3α4, studies using the knock down system for HIF-3α4 would also be required.

Energy in the tumor is produced by a high rate of glycolysis followed by lactic acid fermentation in the cytosol, rather than by a low rate of glycolysis followed by oxidation of pyruvate (Warburg effect), leading to high FDG uptake [24,25]. High FDG/FMISO-uptake in IO-GFP cells tumor (Fig. 3D and E) might be due to constitutive transcriptional activity of HIF-1α, leading to high rate tumor growth and thus high demands for glucose and oxygen. By contrast, IO-HIF3α4 cells tumor grew slower than IO-GFP cells tumor, possibly resulted in lower demand for glucose and oxygen. Thus

FDG and FMISO uptake in IO-HIF3α4 cells kept at low levels. It is very likely that this difference in tumor growth rate caused the difference in overall survival time in the mouse xenograft model (Fig. 3F). From these results, the association between the expression of HIF-3α4 and vascular density or tumor growth in clinical meningioma samples should be examined in future.

In conclusion, present study suggested that overexpression of HIF-3α4 might suppress tumor activities of the meningioma cell line. Although further studies are required, strategies to express high levels of HIF-3α4 could possibly contribute to establish a new treatment for malignant meningiomas.

References

[1] J.Y. Kim, Y.G. Cha, S.W. Cho, E.J. Kim, M.J. Lee, J.M. Lee, J. Cai, H. Ohshima, H.S. Jung, Inhibition of apoptosis in early tooth development alters tooth shape and size, J. Dent. Res. 85 (2006) 530–535.
[2] O. Warburg, On the origin of cancer cells, Science 123 (1956) 309–314.
[3] M. Preusser, M. Hassler, P. Birner, M. Rudas, T. Acker, K. Plate, G. Widhalm, E. Knosp, H. Breitschopf, J. Berger, Microvascularization and expression of VEGF and its receptors in recurring meningiomas: pathobiological data in favor of anti-angiogenic therapy approaches, Clin. Neuropathol. 31 (2012) 352–360.
[4] A. Weidemann, R. Johnson, Biology of HIF-1α, Cell Death Differ. 15 (2008) 621–627.
[5] M.A. Maynard, Human HIF-3 4 is a dominant-negative regulator of HIF-1 and is down-regulated in renal cell carcinoma, FASEB J. 19 (2005) 1396–1406.
[6] T. Tanaka, M. Wiesener, W. Bernhardt, K.U. Eckardt, C. Warnecke, The humanHIF(hypoxia-inducible factor)-3α gene is a HIF-1 target gene and may modulate hypoxic gene induction, Biochem. J. 424 (2009) 143–151.
[7] A. Pasanen, M. Heikkilä, K. Rautavuoma, M. Hirsilä, K.I. Kivirikko, J. Myllyharju, Hypoxia-inducible factor (HIF)-3α is subject to extensive alternative splicing in human tissues and cancer cells and is regulated by HIF-1 but not HIF-2, Int. J. Biochem. Cell Biol. 42 (2010) 1189–1200.
[8] Y. Makino, Inhibitory PAS domain protein (IPAS) is a hypoxia-inducible splicing variant of the hypoxia-inducible factor-3alpha locus, J. Biol. Chem. 277 (2002) 32405–32408.
[9] Y. Makino, R. Cao, K. Svensson, G. Bertilsson, M. Asman, H. Tanaka, Y. Cao, A. Berkenstam, L. Poellinger, Inhibitory PAS domain protein is a negative regulator of hypoxia-inducible gene expression, Nature 414 (2001) 550–554.
[10] M. Heikkil, A. Pasanen, K.I. Kivirikko, J. Myllyharju, Roles of the human hypoxia-inducible factor (HIF)-3ƒ¿ variants in the hypoxia response, Cell. Mol. Life Sci. (2011) 1–17.
[11] J.W. Lee, K.W. Kang, S.H. Park, S.M. Lee, J.C. Paeng, J.K. Chung, M.C. Lee, D.S. Lee, 18F-FDG PET in the assessment of tumor grade and prediction of tumor recurrence in intracranial meningioma, Eur. J. Nucl. Med. Mol. Imaging 36 (2009) 1574–1582.
[12] H. Maier, D. Öfner, A. Hittmair, K. Kitz, H. Budka, Classic, atypical, and anaplastic meningioma: three histopathological subtypes of clinical relevance, J. Neurosurg. 77 (1992) 616–623.
[13] T. Backer-Grøndahl, B.H. Moen, S.H. Torp, The histopathological spectrum of human meningiomas, Int. J. Clin. Exp. Pathol. 5 (2012) 231.
[14] M.K. Aghi, B.S. Carter, G.R. Cosgrove, R.G. Ojemann, S. Amin-Hanjani, R.L. Martuza, W.T. Curry Jr, F.G. Barker, Long-term recurrence rates of atypical meningiomas after gross total resection with or without postoperative adjuvant radiation, Neurosurgery 64 (2009) 56–60.
[15] Y. Kishida, A. Natsume, Y. Kondo, I. Takeuchi, B. An, Y. Okamoto, K. Shinjo, K. Saito, H. Ando, F. Ohka, Epigenetic subclassification of meningiomas based on genome-wide DNA methylation analyses, Carcinogenesis 33 (2012) 436–441.
[16] P.Y. Wen, J. Drappatz, Novel therapies for meningiomas, Expert Rev. Neurother. 6 (2006) 1447–1464.
[17] G.L. Semenza, HIF-1: upstream and downstream of cancer metabolism, Curr. Opin. Genet. Dev. 20 (2010) 51–56.
[18] W.G. Kaelin Jr, P.J. Ratcliffe, Oxygen sensing by metazoans: the central role of the HIF hydroxylase pathway, Mol. Cell 30 (2008) 393–402.
[19] P. Maxwell, G. Dachs, J. Gleadle, L. Nicholls, A. Harris, I. Stratford, O. Hankinson, C. Pugh, P. Ratcliffe, Hypoxia-inducible factor-1 modulates gene expression in solid tumors and influences both angiogenesis and tumor growth, Proc. Natl. Acad. Sci. 94 (1997) 8104.
[20] E. Rankin, A. Giaccia, The role of hypoxia-inducible factors in tumorigenesis, Cell Death Differ. 15 (2008) 678–685.
[21] M.A. Maynard, Multiple splice variants of the human HIF-3alpha locus are targets of the von Hippel–Lindau E3 ubiquitin ligase complex, J. Biol. Chem. 278 (2003) 11032–11040.
[22] G.F. Whitmore, A.J. Varghese, The biological properties of reduced nitroheterocyclics and possible underlying biochemical mechanisms, Biochem. Pharmacol. 35 (1986) 97–103.
[23] D. Bo, S. Laijun, S. Hongwei, Expression of HIF-1, COX-2 and the correlation with angiogenesis in meningioma, Chin. J. Pract. Nerv. Dis. 2 (2008) 005.
[24] J.W. Kim, C.V. Dang, Cancer's molecular sweet tooth and the Warburg effect, Cancer Res. 66 (2006) 8927–8930.
[25] V. Barresi, G. Tuccari, Evaluation of neo-angiogenesis in a case of chordoid meningioma, J. Neurooncol. 95 (2009) 445–447.